

# Improved Accuracy of Actual Flip Angle Imaging (AFI)

K. Nehrke<sup>1</sup>, P. Börner<sup>1</sup>, and U. Katscher<sup>1</sup>

<sup>1</sup>Philips Research Europe, Hamburg, Germany

## Introduction

Accurate  $B_1$  mapping is required for a variety of applications such as quantitative image processing [1] and RF shimming in high-field MRI [2]. Recently, a fast  $B_1$  mapping technique dubbed AFI (actual flip angle imaging, [3]) has been introduced, potentially allowing the in-vivo acquisition of 3D flip angle maps. However, the complete spoiling of transverse magnetization is of crucial importance for the accuracy of this approach. RF phase cycling in combination with diffusion dephasing by means of strong spoiling gradients was proposed, but not quantitatively validated. In the present study, a quantitative analysis of the spoiling properties of the sequence was performed by numerical simulations based on configuration theory. In addition, phantom and in-vivo experiments were performed for comparison.

## Methods

**Simulations:** In configuration theory [4], the magnetization of a pulse sequence is described in terms of coherence (or dephasing) states instead of regarding individual magnetization vectors. This allows the derivation of a recursion relation for the magnetization of the sequence, which may be used for efficient calculation of the steady state signal [5]. In the present work, this concept has been adapted to the AFI sequence and used for the numerical simulation of the AFI steady state signals  $S_1$  and  $S_2$  as a function of the tissue parameters ( $T_1$ ,  $T_2$ , diffusion coefficient  $D$ ) and the sequence parameters ( $TR_1$ ,  $TR_2$ , flip angle  $\alpha$ , spoil phase shift increment  $\phi$  [6], diffusion weighting factor  $b$ ). The simulation has been implemented in C and was used on a standard Pentium PC. To reach steady state,  $3T_1/(TR_1+TR_2)$  iterations were performed.

**Experiments:** Phantom and in-vivo experiments were performed on a clinical 1.5 T MR scanner (Philips Medical Systems, Best, The Netherlands). The AFI sequence was used for imaging of a spherical water phantom ( $64 \times 64$  scan matrix,  $256 \times 256$  mm<sup>2</sup> FOV,  $TR_1=20$  ms,  $TR_2=100$  ms). Acquisitions with different flip angles, spoil phases and  $b$  values were performed. For evaluation, average values of  $S_1$  and  $S_2$  were determined by adding the signal of all pixels in each of the two corresponding images. Subsequently, the flip angle was predicted using the approximation given in [3] and compared with the nominal flip angle calibrated by the system, which was taken as reference. In the in-vivo experiments, 3D  $B_1$  maps of the head were acquired ( $128 \times 81 \times 15$  scan matrix,  $256 \times 162 \times 210$  mm<sup>3</sup> FOV,  $45^\circ$  flip angle,  $TR_1=20$ ms,  $TR_2=100$ ms, 139 s acquisition time, diffusion damping  $b \cdot D = 0.1$ )

## Results

Fig. 1 shows the absolute accuracy of the AFI approach as a function of diffusion damping  $d=D \cdot b$  for different flip angles, relaxation times and spoil phase shift increments  $\phi$ . Simulations and experimental results are shown. For small diffusion damping ( $d < 0.01$ ), large deviations ( $\Delta\alpha > 30^\circ$ ) between actual and predicted flip angle are observed for the two considered values of  $\phi$ . In this range, it was not possible to identify favorable values of  $\phi$ , where accurate flip angle imaging is possible for a reasonable range of flip angles and relaxation times. For medium diffusion damping ( $0.01 < d < 1$ ) in combination with a favorable spoil phase  $\phi=129.3^\circ$ , a good accuracy ( $\Delta\alpha < 2^\circ$ ) is achieved in the studied flip angle range from  $30^\circ$  to  $70^\circ$ . Only for the water signal with its long relaxation times, the deviations slightly increase ( $\Delta\alpha < 6^\circ$ ) for small or large flip angles ( $\alpha = 30^\circ$  or  $\alpha = 70^\circ$ ). In contrast, strong deviations (up to  $35^\circ$ ) are observed for an unfavorable spoil phase  $\phi = 120^\circ$ . In this case, extreme diffusion damping ( $d > 1$ ) is required to ensure accurate flip angle determination. In this range, all transverse coherences are completely spoiled, regardless of the spoil phase. Fig. 2 shows  $B_1$  maps of the head for a selected volunteer. In accordance with the simulations and phantom experiments, a favorable spoil phase  $\phi = 129.3^\circ$  resulted in much smaller deviations from the reference flip angle compared with an unfavorable spoil phase  $\phi = 120^\circ$ .

## Discussion

Simulations based on configuration theory show that the spoiling properties of the AFI sequence may be controlled by the RF spoil phase and the diffusion weighting defined by the spoiling gradients. The selection of a favorable spoil phase allows the gradient spoiling to be reduced significantly without trading the accuracy flip angle imaging. Moreover, the sequence may be adjusted to optimize the accuracy of the maps for a reasonable range of flip angles and tissue parameters, thus improving the robustness and versatility of the technique.

## References

1. Dowell NG, Tofts PS. Magn Reson Med. 2007;58(3):622-30.
2. Katscher U et al. Magn Reson Med. 2003 Jan;49(1):144-50
3. Yarnykh VL. Magn Reson Med. 2007;57(1):192-200.
4. Hennig J. Concepts Magn Reson 1991;3:125-143.
5. Ganter C. Magn Reson Med. 2006 Jan;55(1):98-107.
6. Zur Y et al. Magn Reson Med 1991;21:251-263.

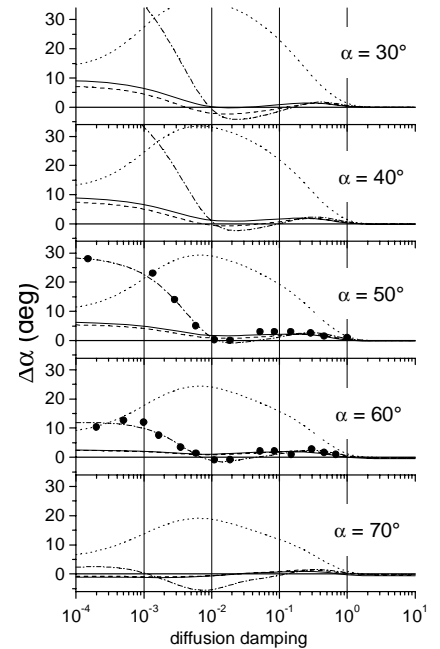


FIG. 1. Accuracy of flip angle imaging. The deviation between predicted and actual flip angle is shown as a function of the diffusion damping value  $d=D \cdot b$  for five different flip angles. Simulations for different  $T_1, T_2$  and  $\phi$  are shown (solid line:  $T_1, T_2, \phi = 10, 7, 129.3^\circ$ , dashed line:  $T_1, T_2, \phi = 60, 7, 129.3^\circ$ , dotted-dashed line:  $T_1, T_2, \phi = 100, 100, 129.3^\circ$ , dotted line:  $T_1, T_2, \phi = 100, 100, 120^\circ$ , relaxation times in units of TR). The solid circles show selected experimental results.

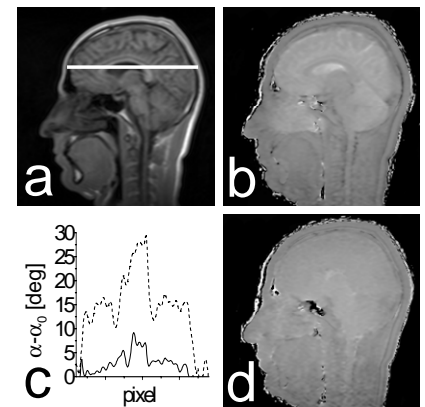


FIG. 2. In-vivo results.  $B_1$  maps of the head are shown for different spoil phases (b:  $\phi = 120^\circ$ , d:  $\phi = 129.3^\circ$ ). The graphs show the difference between predicted and nominal flip angle ( $\alpha_0 = 45^\circ$ ) along a selected profile through the ventricle (indicated by a white line in (a)) for the respective spoil phases (dashed line:  $\phi = 120^\circ$ , solid line:  $\phi = 129.3^\circ$ ).